

MOL #98392

Title page

# **Critical Cysteine Residues in Both the Calcium-Sensing Receptor and the Allosteric Activator AMG 416 Underlie the Mechanism of Action**

Shawn T. Alexander, Thomas Hunter, Sarah Walter, Jin Dong, Derek Maclean, Amos Baruch,  
Raju Subramanian, James E. Tomlinson  
Amgen, Thousand Oaks, CA, USA

MOL #98392

**Running Title:** Mechanism of Action of AMG 416

**Corresponding Author:**

Shawn T. Alexander

Amgen Inc, 1120 Veterans Boulevard

South San Francisco, CA 94080

E-mail: shawna@amgen.com

Tel: +1 (650) 244-2762

Fax: +1 (650) 589-3105

**Document Statistics**

Pages: 42

Tables: 2

Figures: 8

References: 44

Word counts:	Abstract	271
	Introduction	730
	Discussion	1492

**Abbreviations**

CaSR, calcium-sensing receptor; CRR, cysteine-rich region; Cys482, cysteine at position 482; ECD, extracellular domain; ESRD, end-stage renal disease; GPCR, g protein coupled transmembrane receptor; hCaSR, human calcium-sensing receptor; HEK293T, human embryonic kidney 293T; HPLC, high performance liquid chromatography; HPT, hyperparathyroidism; IP-1, Inositol (1) phosphate; LC-MS, liquid chromatography-mass spectrometry; LC-MS/MS, liquid chromatography-tandem mass spectrometry; mGluR, metabotropic glutamate receptor; MRM, multiple reaction monitoring; ORF, open reading frame; pCaSR, pig calcium-sensing receptor; PD, pharmacodynamic; PK, pharmacokinetic; PTH, parathyroid hormone; TASR, taste receptor; TFA, trifluoroacetic acid; VFT, venus fly trap

MOL #98392

## Abstract

AMG 416 is a novel D-amino acid-containing peptide agonist of the calcium-sensing receptor (CaSR) that is being evaluated for the treatment of secondary hyperparathyroidism in chronic kidney disease patients receiving hemodialysis. The principal amino acid residues and their location in the CaSR which accommodate AMG 416 binding and mode of action have not previously been reported. Herein we establish the importance of a pair of cysteine residues, one from AMG 416 and the other from the CaSR at position 482 (Cys482), and correlate the degree of disulfide bond formation between these residues with the pharmacological activity of AMG 416. KP-2067, a form of the CaSR agonist peptide, was included to establish the role of cysteine in vivo and in disulfide exchange. Studies conducted with AMG 416 in pigs showed a complete lack of pharmacodynamic effect and provided a foundation for determining the peptide agonist interaction site within the human CaSR. Inactivity of AMG 416 on the pig CaSR resulted from a naturally occurring mutation encoding tyrosine for cysteine (Cys) at position 482 in the pig CaSR. Replacing Cys482 in the human CaSR with serine or tyrosine ablated AMG 416 activity. Decidedly, a single substitution of cysteine for tyrosine at position 482 in the native pig CaSR provided a complete gain of activity to the peptide agonist. Direct evidence for this disulfide bond formation between the peptide and receptor was demonstrated using a mass spectrometry assay. The extent of disulfide bond formation was found to correlate with the extent of receptor activation. Notwithstanding the covalent basis of this disulfide bond, the observed in vivo pharmacology of AMG 416 showed readily reversible pharmacodynamics.

MOL #98392

## Introduction

AMG 416 (Amgen Inc, Thousand Oaks, CA) is a novel D-amino acid-containing peptide agonist of the calcium-sensing receptor (CaSR) that is currently under investigation for the treatment of secondary hyperparathyroidism (HPT) in patients receiving hemodialysis. AMG 416 acts in a fashion similar to the phenylalkylamine CaSR agonist, cinacalcet (Sensipar<sup>®</sup>/Mimpara<sup>®</sup>, Amgen Inc, Thousand Oaks, CA), by decreasing circulating levels of parathyroid hormone (PTH), calcium and phosphorus in dialysis patients with secondary HPT (Block et al., 2004a; Block et al., 2004b; Lindberg et al., 2005; Martin et al., 2014b; Moe et al., 2005). However, AMG 416 differs from cinacalcet in its chemical class, intravenous (IV) route of administration, extended half-life, and thrice weekly dosing following each hemodialysis session (Martin et al., 2014b). The CaSR, a G-protein coupled transmembrane receptor (GPCR) located on the chief cells of the parathyroid gland, plays an important role in calcium homeostasis. Increased blood calcium levels activate the CaSR, thereby suppressing PTH secretion and synthesis. In contrast, reductions in blood calcium levels reduce CaSR activity, promoting PTH synthesis and secretion. As part of a compensatory mechanism to maintain blood calcium levels within a narrow range, PTH acts on bone to increase bone resorption, and in the kidney to reduce excretion of calcium, which together modulate the amount of calcium entering the bloodstream (Goodman and Quarles, 2008; Rodriguez et al., 2005; Tfelt-Hansen and Brown, 2005). In chronic kidney disease (CKD), functional demand for PTH to rebalance calcium levels frequently leads to the development of secondary HPT (Kidney Disease: Improving Global Outcomes (KDIGO) CKD-MBD Work Group, 2009). Worsening secondary HPT in ESRD patients is often accompanied by parathyroid gland hyperplasia (National Kidney Foundation, 2003). Loss of sensitivity and responsiveness to blood calcium levels in hyperplastic glands, partly as a consequence of downregulated CaSR expression (Komaba et al., 2010), results in dysregulation of PTH secretion and synthesis, and contributes to the excessive PTH levels (Felsenfeld et al., 2007) that are frequently observed in patients with secondary HPT on dialysis.

MOL #98392

The primary pharmacodynamic (PD) effect of calcimimetics is to reduce PTH levels, either by lowering the threshold for CaSR activation in response to extracellular calcium, and/or by directly activating the CaSR itself (Nemeth et al., 1998). Reductions in calcium are a secondary PD effect of calcimimetics and are influenced by reductions in PTH (Chen and Goodman, 2004; Mundy and Guise, 1999). The first commercially-available calcimimetic, cinacalcet, is an allosteric activator of the CaSR that lowers the threshold for activation by the orthosteric agonist, calcium. Cinacalcet decreases PTH, as well as calcium and phosphorus, in ESRD patients with secondary HPT (Block et al., 2004b; Lindberg et al., 2005; Moe et al., 2005). Although cinacalcet is approved as a once-daily oral treatment for secondary HPT in CKD patients on dialysis, its use is limited by gastrointestinal side effects that include nausea, vomiting, and diarrhea (Sensipar Prescribing Information [Amgen Inc]), restricted opportunity to titrate doses due to fixed dosage form and strength, cytochrome P450-mediated drug-drug interactions (Padhi and Harris, 2009), and diminished patient adherence (Gincherman et al., 2010). Consequently, an alternative calcimimetic therapy for secondary HPT is warranted.

AMG 416 is a synthetic 8-amino acid peptide calcimimetic that activates the CaSR in the presence of extracellular calcium in vitro, but also demonstrates lower activity when extracellular calcium is absent (Walter et al., 2013). AMG 416 administration leads to dose-dependent suppression of PTH in normal and uremic rats (Walter et al., 2013), healthy adults (Martin et al., 2014a), and patients with secondary HPT on hemodialysis (Martin et al., 2014b). AMG 416 also reduces serum phosphorus and calcium levels in patients with secondary HPT on hemodialysis (Martin et al., 2014b).

The current study was undertaken to examine the mechanism of action of AMG 416. Early studies showed reductions in PTH and calcium following exposure to AMG 416 in rats, dogs, and humans, but similar PD effects were not observed in pigs. We hypothesized that there are

MOL #98392

one or more key amino acids in the CaSR from responsive species that govern AMG 416 activity and that are mutated in the pig. Through studies involving determination of the pig CaSR sequence, comparisons to CaSR sequences from responsive species, receptor activation measures with mutated forms of the receptor, and mass spectrometry methods, we have identified a critical interaction between AMG 416 and the CaSR. We will discuss the relevance of this interaction for observed pharmacological activities of AMG 416.

MOL #98392

## **Materials and Methods**

All animal studies were performed according to Institutional Animal Care and Use Committee guidelines and approved by each institution that conducted the studies.

### ***Peptide Synthesis and Sequences***

Peptides AMG 416 (Ac-c[C]arrar-NH<sub>2</sub>; 1048 Da), KP-2067 (Ac-carrar-NH<sub>2</sub>; 929 Da), and KP-2140 (Ac-arrar-NH<sub>2</sub>; 826 Da) were synthesized using the methods as described previously (Walter et al., 2013). Lower case letters in sequences represent D-amino acids while upper case is an L-amino acid.

### ***Pharmacology Studies in Normal Rats***

Male Sprague Dawley rats with weights averaging 300 g (Charles River Laboratories International, Wilmington, MA) were administered either 3.0 mg/kg KP-2140, 3.0 mg/kg KP-2067, 0.5 mg/kg KP-2067, or saline via IV bolus. Blood samples were collected at 1, 2, 3, and 4 hours post dose and plasma PTH was quantified using a Rat Bioactive Intact PTH ELISA (Cat. #60-2700; Immutopics International, San Clemente, CA) in accordance with the manufacturer's protocol. Two-way analysis of variance (ANOVA) was used to determine statistical significance with Bonferroni adjustment for multiple comparison (GraphPad Prism v6.03; GraphPad, La Jolla, CA).

### ***Pharmacology Studies in Normal Dogs***

#### ***Single IV Bolus***

This study was conducted by Charles River Laboratories, (Reno, NV). Male beagle dogs aged 12 months with weights ranging from 10.5 to 11.9 kg were administered 1.5 mg/kg AMG 416 via IV bolus. Blood samples were collected pre-dose and every 3 hours post dose administration for up to 48 hours to determine plasma AMG 416, PTH, and total calcium concentrations. Plasma concentrations of AMG 416 were quantified following an ion-exchange solid-phase extraction

MOL #98392

procedure by liquid chromatography – tandem mass spectrometry (LC-MS/MS). LC separations were performed by reverse phase HPLC (Beta Basic C<sub>18</sub> column; 2.1 mm × 50 mm; Thermo Fisher Scientific, Inc, Waltham, MA) using 0.07% TFA/0.1% formic acid and acetonitrile as mobile phase. Analyte detection was performed with a multiple reaction monitoring method in the positive ion mode on a triple quadrupole mass spectrometer (API; AB Sciex, Framingham, MA). Plasma PTH was determined using the manufacturer's protocol with a Canine Intact PTH ELISA kit (Cat. # 60-3800; Immutopics International). Total calcium was quantified using a Beckman SYNCHRON CX7<sup>®</sup> Automated Chemistry Analyzer. Statistical significance was determined by two-way Analysis of Variance (ANOVA) with Bonferroni adjustment for multiple comparison (GraphPad Prism v6.03).

#### ***Twenty-four Hour IV Infusion***

Study was conducted by ITR Laboratories Canada Inc, (Baie d' Urfé, Québec, Canada). A single group of male beagle dogs aged 14 to 16 months with weights ranging from 7.6 to 10.9 kg were sequentially administered vehicle (20 mM succinate with 0.81% sodium chloride; pH 4.5 to 4.6), AMG 416 at 0.192 mg/kg (8 µg/kg/hr), and then AMG 416 at 0.48 mg/kg (20 µg/kg/hr) via 24-hour IV infusion, with a 1-week washout period between dose groups. The same dogs were used throughout the study to minimize the use of animals and to reduce variability between treatment groups. Blood samples were collected at pre-dose, 4, 8, 12, 16, 20 and 24 hours after the start of infusion, and at 1, 3, 6, 12, 18 and 24 hours after the end of infusion to determine total calcium, plasma PTH, and AMG 416 plasma concentrations. Statistical analysis and plasma concentrations of AMG 416 and PTH were determined as described in the dog single IV bolus study. A Roche/Hitachi 912 Biochemistry Analyzer using o-cresolphthalein complexone was used to quantify total calcium.



MOL #98392

### ***Pharmacology Studies in Normal Pigs***

Study was conducted by Avanza Laboratories, (Gaithersburg, MD). Male Gottingen minipigs with weights ranging from 8.9 to 11.2 kg were administered either 0.3 mg/kg, 1 mg/kg, or 5 mg/kg AMG 416 via IV bolus. Blood samples were collected at pre-dose, 0.08, 2, 4, 8, 12, 18, 24, 36, and 48 hours post-dose administration to determine total calcium and AMG 416 plasma concentrations. Plasma concentrations of AMG 416 were measured as described for the dog studies. Two-way ANOVA was used to determine statistical significance with Bonferroni adjustment for multiple comparisons.

### ***Pig CaSR DNA Sequence Determination***

Complete sequencing of the pig CaSR DNA was performed by Abgent Inc (San Diego, CA) and is further detailed in **Supplemental Figure 1**. Pig CaSR sequence has been deposited in GenBank with accession number KT309043.

### ***DNA Constructs for Wild Type and Mutant CaSRs***

Native and mutant CaSR expression constructs were synthesized as open reading frames (ORFs) and sub-cloned into a mammalian expression vector (vector pJ609; DNA 2.0, Inc; Menlo Park, CA). Each ORF contained an amino-terminal leader sequence, followed by a FLAG epitope tag, linked to the first amino acid (tyrosine) normally found in the mature native CaSR. All amino acid position designations (eg, 482) were with respect to the native (non-tagged) human CaSR (hCaSR) sequence. Only a single residue substitution was made relative to the native amino acid sequence for each mutant construct. Constructs expressed and analyzed in these studies were: (1) native hCaSR, which encodes a cysteine at position 482 (C482); (2) mutant hCaSR (C>Y482; a tyrosine substitution for the wild type cysteine at position 482); (3) mutant hCaSR (C>S482; a serine substitution for the wild type cysteine at position 482). (4) native pig CaSR (pCaSR), which encodes a tyrosine at position 482 (Y482); and (5) mutant

MOL #98392

pCaSR (Y>C482; a cysteine substitution for the wild type tyrosine at position 482). All CaSR constructs were completely sequenced and confirmed by DNA 2.0, Inc.

### ***Expression and Analysis of DNA Constructs***

Human embryonic kidney (HEK293T) cells were transiently transfected with Lipofectamine (Life Technologies, Carlsbad, CA) and one CaSR construct per transfection. For any given transfection session each of the CaSR constructs listed in either Figure 3 or 4 were run in parallel. A separate transfection was run on a different date for each of four (unless otherwise noted) replicates. Following transfection, cells were re-plated at 32-34 hours in Dulbecco modified eagle medium (Life Technologies) supplemented with 10% heat inactivated fetal bovine serum and 2 mM L-glutamine and assayed for IP-1 production at 48 hours.

### ***Analysis of KP-2067 and KP-2140 in a Stable Cell Line Expressing hCaSR***

Dose response curves for KP-2067, KP-2140 and calcium were measured in a clonal cell line of HEK293T stably transfected with the human CaSR (Multispan; Hayward, CA) and as previously described for AMG 416 (Walter et al., 2013).

### ***Inositol-1-Phosphate (IP-1) Production in HEK293T Cells Expressing CaSR***

CaSR activation was measured in vitro by quantifying the accumulation of IP-1, a surrogate of inositol (1,4,5) triphosphate production and Gq stimulation, as previously described (Walter et al., 2013) with the following modification: 500  $\mu$ M 2-mercaptoethanol was added to the base stimulation buffer for AMG 416 but not for calcium, KP-2067, or KP-2140. This concentration of 2-mercaptoethanol was chosen based on previous studies that provided optimal AMG 416 activity, yet had no measurable effect on stimulation of the hCaSR by either calcium or KP-2067.

MOL #98392

Each replicate is a mean value of IP-1 measured independently in 4 separate wells. Mean IP-1 values from each replicate were entered individually in Prism (GraphPad Prism v6.03;) and mean  $\pm$  S.E.M. were plotted.

### ***Determination of Fractional Occupancy of CaSR by Agonist Peptide***

#### ***Ligand Binding to the CaSR***

A clonal cell line of HEK293T stably transfected with the human CaSR (Multispan) was grown to 90% confluence in glutathione-free RPMI-1640 media (Life Technologies) supplemented with 10% heat inactivated fetal bovine serum, 2 mM L-glutamine, and 1  $\mu$ g/mL puromycin. Cells were washed with  $\text{Ca}^{2+}/\text{Mg}^{2+}$  free-PBS, dislodged with 500  $\mu$ M EDTA, and following a wash with  $\text{Ca}^{2+}/\text{Mg}^{2+}$  free-PBS and complete aspiration, resuspended in base stimulation buffer (Walter et al., 2013) containing 1.2 mM  $\text{Ca}^{2+}$ . Cell suspensions were incubated with vehicle (saline) or KP-2067 at 8  $\mu$ M ( $\text{EC}_{20}$ ), 25  $\mu$ M ( $\text{EC}_{50}$ ), or 80  $\mu$ M ( $\text{EC}_{80}$ ) for 30 minutes at 37°C with constant inversion. Cells were washed with cold base stimulation buffer, aspirated completely and then lysed with 20 mM phosphate-citrate buffer (pH,6) containing 0.5% NP-40, 150 mM NaCl, 1mM EDTA, and 1x Roche Complete Mini Cocktail (Cat # 04 693 124 001; Roche Diagnostics). Lysates were centrifuged twice at 4°C for 10 minutes at 14,000  $\times$  g and the pellet was harvested.

The pellet was reconstituted in a digestion buffer containing 4 M urea, 50 mM ammonium bicarbonate stock (pH 6), and ProteaseMax (# V2072; Promega, Madison, WI). Free sulfhydryl groups were modified by the addition of acrylamide (0.1M) followed by a 30 minute incubation at room temperature. Samples were proteolyzed by the addition of sequencing grade chymotrypsin (Cat # 11418467001; Roche). The digest reaction was quenched by acidification with 1% formic acid and insoluble material was removed by centrifugation. This chymotryptic digested mixture was analyzed by liquid chromatography-tandem mass spectrometry (LC-MS/MS).

MOL #98392

### ***Mass Spectrometric Analysis of Ligand Binding to the hCaSR***

Ligand-receptor adducts were monitored by LC-MS/MS. Peptide standards representing the putative cysteine-containing chymotryptic peptides of the CaSR were synthesized and reacted with either KP-2067 to represent the disulfide pair with ligand, or with acrylamide to represent the unmodified free sulfhydryl form of CaSR. The resulting synthetic conjugates were infused into the triple quadrupole mass spectrometer (TSQ Quantum Ultra; Thermo Fisher Scientific, San Jose, CA) and electrospray ionization was performed in the positive ion mode. The resulting ions were subjected to collision-induced dissociation and secondary (MS/MS) spectra were acquired to identify the fragmentation pattern for each conjugate. Representative MS/MS spectra of acrylamide-modified and KP-2067/ CaSR (DECGDL) peptide conjugates are shown in **Figure 5**. The fragmentation data (precursor ion  $m/z$ , collision energy, and product ion  $m/z$ ) from these standards were used to identify the corresponding species from multiple reaction monitoring (MRM) assay of peptide digest samples from cellular assays.

Chromatographic separation of the chymotrypsin digests was performed by reversed-phase HPLC on an Agilent 1100 system. A reverse-phase column (Bio-Basic C18, 5  $\mu$ M, 2.1 $\times$ 50 mm; Thermo Fisher Scientific) maintained at 40°C was employed. The mobile phase flowing at 400  $\mu$ L/min was comprised of 0.1% trifluoroacetic acid (TFA) in water (solvent A), and 0.1% TFA in acetonitrile (solvent B). The solvent gradient was as follows: 0 to 1 min, 100% A; 1 to 5 min, 100% to 20% A; 5 to 6 min, 20% A; 6 to 7 min, 20% to 100% A; 7 to 10 min, 100% A. The total run time was 10 min.

Analyte detection was performed in the positive ion mode employing a multiple reaction mode method on a triple quadrupole mass spectrometer (TSQ Quantum Ultra). The monitored mass transitions were as follows: acrylamide-modified DECGDL,  $m/z$  722.2  $\rightarrow$   $m/z$  146.7 & 346.8 and DECGDL-KP-2067 conjugate,  $m/z$  789.9  $\rightarrow$   $m/z$  448.2 & 464.2. Under these conditions, the

MOL #98392

acrylamide-modified CaSR peptide eluted at 4.88 min and the KP-2067/CaSR peptide conjugate eluted at 5.02 min. All data were acquired and processed using Xcalibur software (Thermo Fisher Scientific) and peak areas were computed from the MRM chromatograms.

The MS responses for the CaSR peptide bound to both acrylamide and KP-2067 were assumed to be the same. The fractional occupancy of KP-2067 was computed as follows:

$$\text{Fractional occupancy (\%)} = 100 \times \frac{\text{Peak Area}_{\text{KP2067}}}{\text{Peak Area}_{\text{acrylamide}} + \text{Peak Area}_{\text{KP2067}}}$$

The subscripts acrylamide and KP-2067 represent the species conjugated to the CaSR peptide.

MOL #98392

## Results

### *The Role of Cysteine in the Peptide Agonist for Activation of the CaSR*

#### *In Vitro hCaSR Studies*

Three synthetic peptides were selected to help elucidate the critical components required for hCaSR activation (**Figure 1A**). AMG 416 is a D-amino acid peptide containing an N-terminal cysteine residue disulfide linked to L-cysteine (sequence structure = Ac-c[C]arrar-NH<sub>2</sub>). KP-2067 is a structurally related peptide (Ac-carrar-NH<sub>2</sub>) in which the N-terminal D-cysteine residue is unconjugated and carries a free sulfhydryl group. KP-2140 (Ac-arrar-NH<sub>2</sub>) does not have a cysteine at the N-terminus. Each peptide contained the identical arginine-alanine composition and spacing that is found in the D-peptide backbone of AMG 416.

A clonal cell line of HEK293T overexpressing the hCaSR was used to examine the responses to the CaSR orthosteric ligand, calcium, and the peptides KP-2067 and KP-2140 (**Figure 1A**). The peptide dose-response curves were each run in the presence of 1.2 mM calcium. The EC<sub>50</sub> for calcium was calculated to be  $4.6 \pm 0.04$  mM, within the range of published values (Breitwieser and Gama, 2001; Conigrave et al., 2004; Wei et al., 2014). The measured EC<sub>50</sub> for KP-2067 was  $18.4 \pm 0.07$   $\mu$ M, and the calculated Hill coefficient was  $1.5 \pm 0.33$  similar to the reported values of 25  $\mu$ M and 1.1, respectively, for AMG 416. These Hill coefficients are consistent with a single binding site for agonist peptide on the CaSR. The dose response curve for calcium was steeper than that for KP-2067, with a Hill coefficient of 3 to 4, consistent with the presence of multiple binding sites for calcium on the CaSR (Wei et al., 2014). In contrast, IP-1 levels remained at or near baseline value when incubated with KP-2140. The mean maximal IP-1 induction for KP-2067 was 29-fold higher than the baseline value.

MOL #98392

### ***Rat Pharmacodynamic Studies with Peptides***

IV bolus administration of KP-2067 at 3 mg/kg and 0.5 mg/kg significantly reduced plasma PTH to below 5% of pre-dose values at one hour after dosing (**Figure 1B**). At 4 hours post-dose, the mean plasma PTH levels in rats administered 3 mg/kg and 0.5 mg/kg KP-2067 were  $4.6 \pm 0.9\%$  ( $P < 0.05$ ) and  $36.6 \pm 15.3\%$  ( $P < 0.001$ ) of pre-dose values, respectively. Mean plasma PTH levels for rats dosed with 3 mg/kg KP-2067 were significantly different ( $P < 0.001$ ) from the saline control group at all measured time points. KP-2140 dosed at 3 mg/kg resulted in no significant change from pre-dose plasma PTH values throughout the 4-hour study, and did not differ significantly from saline control.

### ***Dog and Pig PK/PD Studies with AMG 416***

Preliminary PK/PD relationships were established in dogs following administration of a single 1.5 mg/kg AMG 416 IV bolus dose. Plasma concentrations of AMG 416 were highest at the first measured time point post-dose (3 hours) and decreased gradually over 48 hours (**Figure 2A**). Total serum calcium decreased to  $68 \pm 1.6\%$  of pre-dose values ( $P < 0.001$ ) at 24 hours after dosing, and returned to  $89.7 \pm 0.5\%$  of pre-dose values ( $P < 0.001$ ) at 48 hours after dosing (**Figure 2B**). PTH also declined in dogs dosed with AMG 416 (**Supplemental Figure 2**).

AMG 416 was detected in all plasma samples from pigs dosed with AMG 416. Plasma concentrations were consistent within dose groups with minimal inter-animal variation (**Figure 2C**). AMG 416 dose-PK exposure relationships were similar between the dog and pig (compare **Figures 2A** and **2C**). Serum calcium levels did not change significantly over the sampling period, thus showing an absence of AMG 416 PD effect in pigs (**Figure 2D**). This absence of an AMG 416 effect in pigs (even at a very high dose of 5.0 mg/kg) contrasts with results observed for normal dogs, rats, and humans. Data for dogs (**Figure 2B**) at 9 hours following a dose of AMG 416 at 1.5 mg/kg show reduction in total blood calcium of  $19.0 \pm 1.4\%$  (mean  $\pm$

MOL #98392

S.E.M.) ( $P < 0.001$ ; paired Student's  $t$ -test) relative to pre-dose values. Data from rats (Walter et al., 2013) describe significant reductions in total blood calcium at 8 hours relative to pre-dose (mean  $\pm$  S.E.M.) values of  $6.2 \pm 0.8\%$ ,  $12.3 \pm 0.6\%$ ,  $25.2 \pm 1.3\%$  (all  $P < 0.0001$ ; paired Student's  $t$ -test) for 0.3 mg/kg, 1 mg/kg, and 3 mg/kg dose groups, respectively. Lastly, data from healthy young male human subjects (Martin et al., 2014a) show significant reductions in blood ionized calcium levels of  $16.3 \pm 1.0\%$  (mean  $\pm$  S.E.M.;  $P < 0.0001$ ; paired Student's  $t$ -test) at 9 hours following an IV dose of 5 mg AMG 416 relative to pre-dose values. The absence of a PD response in pigs, in the presence of a normally effective exposure level of AMG 416, led to further investigations into the cause.

### ***The Role of Cysteine 482 in the CaSR for Activation by AMG 416 Sequence and Topology of the Pig CaSR***

The pig CaSR (pCaSR) was completely sequenced to explore whether the lack of PD response to AMG 416 in pigs was associated with receptor composition. The entire 3240-nucleotide open reading frame (ORF) of the pCaSR encodes 1079 amino acids and a stop codon (**Supplemental Figure 1**). This sequence has been deposited into GenBank with accession number KT309043.

As is typical of Class C GPCRs (Conigrave and Hampson, 2010), the mature (surface-expressed) pCaSR contains 3 major domains: the large extracellular domain (ECD; 587 amino acids), the heptahelical or transmembrane domain (245 amino acids), and the cytosolic or intracellular domain (228 amino acids). Two of the three CaSR domains are highly conserved (> 90%) across the four species receiving AMG 416 (human, rat, dog, pig) with amino acid identities of 94.7% in the ECD and 97.7% in the heptahelical domain, but a lessened 73.8% conservation in the cytosolic domain. The ECD is further comprised of two subdomains: the



MOL #98392

amino terminal Venus fly trap (VFT) containing 509 amino acids and the carboxy-terminal cysteine-rich region (CRR) containing 78 amino acids.

### ***Candidate Ligand Binding Residues: Amino Acids Not Found in the Pig***

**Table 1** shows all 9 amino acid residues that are unique to the pCaSR ECD which are not found in the CaSR ECD from human, dog or rat. All of these residues are located within the VFT subdomain. Of particular note was the tyrosine at position 482 in the pCaSR (numbering per hCaSR) instead of the equivalent cysteine in the CaSR of each of the species which respond to AMG 416. There are 19 orthologous cysteines in the CaSR ECD of all responsive species (10 in the VFT and 9 in the CRR). Due to a tyrosine at position 482, pigs have only 18 of the otherwise orthologous cysteines. Cysteine in the CaSR is a logical binding partner to the critically important cysteine in the agonist peptide. Therefore, investigations focused on cysteine 482.

### ***DNA Construct Studies - Cys482 and CaSR Activation***

Replacing cysteine at position 482 in the hCaSR with either tyrosine or serine eliminated activation by peptide agonists but did not affect the response to the orthosteric ligand, calcium (**Figure 3A**). The CaSR responses to peptide agonists KP-2067 (**Figure 3B**) and AMG 416 (**Figure 3C**) differed among the three receptor constructs. A cysteine at position 482 was required for peptide agonist activation of the hCaSR. Peptide agonists were not active when cysteine 482 was replaced by either serine (conservative substitution) or tyrosine (the native residue in pigs). In contrast, **Figure 3A** shows that responses to calcium were similar among transfectants for each of three CaSR constructs: native human CaSR (Cys482); one mutant human CaSR (Tyr482); and a second mutant human CaSR (Ser482). Expression analysis using immunostaining of the FLAG epitope and flow cytometry analysis corroborated the calcium activation data and showed similar levels of expression for each construct (**Supplemental Figure 3**).

MOL #98392

To test whether cysteine at position 482 is sufficient to provide a gain of activation of the pCaSR to agonist peptide, the full pCaSR was studied with either a native (tyrosine) or substituted (cysteine) residue at position 482. All of the other amino acid residues in the native pCaSR ORF were maintained. Native human CaSR was used as a positive control for each transfection experiment. **Figure 4A** shows that calcium responses among each of the two pCaSR constructs were largely indistinguishable from that of the hCaSR, and that either tyrosine or cysteine at position 482 in pCaSR led to a normal response to the orthosteric ligand, calcium. Expression analysis using FLAG confirmed similar levels of expression for each construct. (**Supplemental Figure 4**). Despite the normal in vitro response to calcium, native pCaSR (with tyrosine) was not activated by KP-2067 (**Figure 4B**) or AMG 416 (**Figure 4C**). However, complete activation of the pCaSR by both AMG 416 and KP-2067 was gained by simply substituting a cysteine at position 482 in the native pig sequence. The degree of mutant pCaSR (with Cys482) activation by agonist peptide was indistinguishable from activation seen with the hCaSR (**Figures 4B and 4C**). Surface expression levels of CaSR determined by FACS analysis was also similar among the constructs used in these studies (**Supplemental Figure 4**).

#### ***Identifying the Presence of a Disulfide Linkage in the Human CaSR Peptide Conjugate***

Agonist peptide products quantified by MS-MS in these studies are consistent with the presence of a disulfide bond between the peptide and the CaSR. The proposed structures of the CaSR products and the dissociation mechanisms of the D-peptide as a disulfide conjugate with a L-cysteinyl peptide (or L-cysteine) are shown in **Figure 5B**, with a representative mass spectrum. Under MS-MS conditions the protonated peptide conjugate yields major products resulting from sulfur-carbon (S-C) and sulfur-sulfur (S-S) bond cleavages. The major product ion for the KP-2067/CaSR peptide conjugate was  $m/z$  448.33; the ion was formed upon loss of sulfur and led to formation of a dehydroalanine analog of KP-2067. The product ion seen with  $m/z$  464 was the result of S-S bond cleavage in the disulfide conjugate, while the product ion at  $m/z$  481 was

MOL #98392

formed from S-C cleavage in the DECGDL peptide from the CaSR (chymotryptic peptide 480-485). The DECGDL peptide which is unmodified by agonist peptide was characterized following modification of the cysteine with acrylamide. This peptide is shown in **Figure 5A**, with a representative spectrum.

### ***Occupancy of hCaSR Cysteine 482 is Proportional to Concentrations of Peptide Ligand***

HEK293 cells expressing the hCaSR were incubated with KP-2067 at concentrations reflecting the EC<sub>20</sub> (8  $\mu$ M), EC<sub>50</sub> (25  $\mu$ M) and EC<sub>80</sub> (80  $\mu$ M) (**Figure 1A**). Binding of KP-2067 to cysteine 482 was monitored by using multiple reaction monitoring (MRM) mass spectrometry. The disulfide nature of the linkage was confirmed by the formation of the dehydroalanine ligand product after collisional activation of peptide conjugates in the mass spectrometer. Fractional occupancy (% Bound) was determined by comparing the relative abundance of disulfide linked cysteine 482 to the sum of both acrylamide-modified (unbound) cysteine 482 and bound (agonist peptide disulfide linked) fragments liberated after chymotryptic digestion. Both peptide conjugates were analyzed simultaneously by LC-MS/MS from a single sample. The results from this analysis are summarized in **Table 2**.

Other cysteine residues at positions 101, 358, 395, 541, 545, and 598 in the ECD of the hCaSR exhibited only low, variable levels of modification by KP-2067. For all of these other cysteines, modification by agonist peptide corresponded to fractional occupancy less than 1% at the EC<sub>80</sub> peptide concentrations, was not seen in all replicate experiments, and no binding was observed at EC<sub>20</sub> or EC<sub>50</sub> levels. This degree of modification is consistent with nonspecific binding of agonist peptide.

### ***AMG 416 Exhibits Readily Reversible Pharmacodynamics***

Dogs were infused for 24 hours with vehicle or AMG 416 at either 0.192 mg/kg (8  $\mu$ g/kg/hr; n = 4) or 0.480 mg/kg (20  $\mu$ g/kg/hr; n = 4). Steady state levels of AMG 416 were reached by the end

MOL #98392

of infusion for both doses and declined thereafter (**Figure 6A**). Plasma concentration of AMG 416 was dose-dependent, as indicated by an average of  $2.5 \pm 0.1$ -fold difference between doses over the course of the infusion. Plasma PTH levels were inversely correlated with AMG 416 plasma concentrations. Although at times plasma PTH levels showed substantial inter-animal variability in the vehicle control, AMG 416 still produced significant reductions in PTH when compared to vehicle after the start of infusion: 0.480 mg/kg dose, at 2, 8, 12 and 16 hours ( $P < 0.05$ ; 0.192 mg/kg dose, at 12 hours ( $P < 0.05$ ). Plasma PTH began to return to pre-infusion levels immediately following the end of infusion, and was inversely correlated with AMG 416 plasma levels (**Figure 6B**).

At 12 hours post initiation of infusion, total calcium decreased by approximately 3.8% and to 9.8% ( $P < 0.01$ ), with 0.192 mg/kg and 0.480 mg/kg AMG 416 doses, respectively, relative to pre-infusion values (**Figure 6C**). Maximal AMG 416-induced calcium reductions relative to pre-infusion values were 12.9% ( $P < 0.001$ ) with 0.192 mg/kg at 25 hours and 23.4% ( $P < 0.001$ ) with 0.480 mg/kg at 24 hours. Total calcium for the 0.480 mg/kg AMG 416-dosed group differed significantly ( $P < 0.05$ ) from that of the vehicle-dosed group at every time point evaluated after the start of infusion. Significant differences ( $P < 0.05$ ) in total calcium between the 0.192 mg/kg AMG 416-dosed group and vehicle-group were observed at 12 hours post start of infusion through 36 hours.

### ***CaSR Cysteine 482 and Other Related GPCRs***

#### ***GPCR Alignment***

There are 23 independent Class C GPCRs, some with known functions (2 receptors which are activated by calcium [CaSR, GPRC6a], 8 metabotropic glutamate receptors [mGluR<sub>1-8</sub>], 3 taste receptors [TAS1R<sub>1-3</sub>], and a mouse pheromone receptor [V2R] which does not appear to have a human counterpart), and others with orphan status (GPR156, GPR158, GPR179,

MOL #98392

GPRC5A/RAIG1, GPRC5B/RAIG2, GPRC5C/RAIG3, GPRC5D/RAIG4). Two other gene products considered members of the Class C GPCR family are the GABA B1 and GABA B2 subunits, which together form the heterodimeric GABA<sub>B</sub> receptor. All but the orphan members of the Class C GPCR family have a large VFT domain, and all but the GABA B1 and B2 subunits have an additional CRR located between the amino terminal VFT domain and the heptahelical transmembrane domain (IUPHAR/BPS Guide to Pharmacology: G Protein-Coupled Receptors, 2014; Pawson et al., 2014). A regional view of an amino acid alignment from all human GPCRs having a VFT was completed which focuses on the third inter-lobe hinge strand, and cysteine 482 of the CaSR (**Figure 7**). First, using full-length human ORFs, a global alignment grouped the VFT and CRR, as well as the heptahelical and intracellular domains of every GPCR with a known VFT in the extracellular domain. A more refined alignment of the third strand in the hinge of the VFT was subsequently generated using three main refinement criteria: 1) Each VFT is in strict register with the downstream CRR, with good alignment of the 9 cysteines within those subdomains (alignment view not shown). Exception: GABA B subunits do not have a CRR; 2) structural information for 4 independent members of the Class C GPCRs demonstrated identical positioning of landmarks in three dimensional space within the alignment (see boxes within columns 1, 3, 5, and 7); 3) Alignment of highly conserved residues was observed within the third hinge strand, which included two entirely conserved phenylalanines (columns 2 and 4) and a largely conserved glycine-anion dipeptide (column 6).

Cysteine 482 is within the apex of a second turn in the third hinge strand commonly found in all four Class C GPCR structures. This hinge region is also very near the proposed location for the high affinity calcium binding site in the CaSR (Huang et al., 2009). Examination of all other Class C GPCRs with VFTs indicates that none of them contains a cysteine in this same hinge region.

MOL #98392

To support the location of Cys 482 based on the alignment-based model, an independent structural model of the hCaSR was developed. This model also places Cys482 in the third hinge strand of the human CaSR (**Figure 8**).

MOL #98392

## Discussion

Stimulation of the CaSR by AMG 416 requires cysteines in both the agonist peptide and the CaSR. The requirement for a cysteine in the agonist peptide was independently determined from head-to-head comparisons with KP-2067 and KP-2140 using both in vitro CaSR activation measures and in vivo PD assessments. While KP-2067 provided dose-dependent activation of the CaSR, KP-2140 was completely inactive in an in vitro system and did not exhibit calcimimetic behavior. Administration of KP-2067 in normal rats led to rapid reductions in PTH levels, whereas KP-2140 neither suppressed PTH levels in vivo, nor displayed calcimimetic properties. Thus for CaSR activation, this class of calcimimetic requires a cysteine at the amino terminus of the D-amino acid peptide.

KP-2067 was included to aid understanding of AMG 416 mechanism of action for two important reasons: 1) KP-2067 is more structurally similar to the non-cysteine containing peptide KP-2140 than AMG 416 for establishing the role of the peptide cysteine in CaSR activities; 2) We know that the agonist peptide (whether KP-2067 or AMG 416) must contain a cysteine, which is able to accommodate disulfide exchange. All observations made in vivo are consistent with a highly dynamic redox environment that is dependent on a number of disulfide donors and acceptors (the complexity of which we are unable to reproduce in vitro). In vivo KP-2067 is rapidly converted to AMG 416 and AMG 416 undergoes disulfide exchange to form mixed disulfides. These observations are the subject of an upcoming publication. The PD effects of KP-2067 and AMG 416 appear to work by the same mechanism of action in vivo, perhaps with KP-2067 being converted first to AMG 416. Maximal in vitro activation of the CaSR requires a reducing agent (such as beta-mercaptoethanol) for AMG 416, but not for KP-2067 (data on file at Amgen). In vitro reducing agents affect both the disulfide status of AMG 416 and the receptor-agonist peptide interaction. Receptor pull down experiments with agonist peptide are ineffective with reducing agents, but work well when reducing agents are excluded (data on file

MOL #98392

at Amgen). These observations are consistent with the requirement of a disulfide bond between KP-2067 and Cys 482 of the CaSR and the dependence on Cys 482 for both KP-2067 and AMG 416 activity.

The requirement for a cysteine in the CaSR was confirmed by additional studies. First, pigs did not demonstrate a PD response even at exposure levels of AMG 416 that elicited strong responses in dogs, rats and humans. Second, a CaSR lacking a cysteine at position 482 was not activated by either AMG 416 or KP-2067 in vitro. This was observed both for the hCaSR after replacing the native cysteine at position 482 with either serine or tyrosine, and for the native pCaSR which has tyrosine at position 482. Third, the response of native pCaSR to both AMG 416 and KP-2067 in vitro was entirely influenced by simply replacing tyrosine with cysteine at position 482 in the pCaSR. The absence of native pCaSR activation by AMG 416 or KP-2067 in vitro correlated with the lack of a calcimimetic effect observed in pigs with AMG 416 in vivo. A mutated CaSR, with substitutions of either tyrosine or serine at position 482, was not stimulated by AMG 416, but was fully activated by the orthosteric ligand, calcium. This finding indicates that AMG 416 is an allosteric activator of the CaSR with the CaSR binding site distinct from calcium.

Many naturally occurring mutations have been described in the ECD of the CaSR which either increase or decrease the potential for receptor activation (Hu and Spiegel, 2007). In the VFT domain alone there are over 20 independent inactivating mutations which lead to decreased CaSR activation. Most of these mutations are to amino acid residues that are distinct from those believed to bind directly to calcium or other natural CaSR agonists (Huang et al., 2009; Huang et al., 2007; Khan and Conigrave, 2010; Zhang et al., 2014; Zhang et al., 2002). With the CaSR demonstrating a tendency for a high degree of inactivating mutations that are not directly involved in ligand binding, it is possible that substitutions for cysteine 482 would also fall within this class of mutations. To differentiate between direct or indirect influences of cysteine 482 on



MOL #98392

activity of AMG 416 we quantified a direct interaction between the agonist peptide and cysteine 482 by disulfide bond formation and determined that the extent of this interaction correlated with pharmacological activity. Under conditions of increasing ligand exposure and elevated CaSR activity, agonist peptide demonstrated increased fractional occupancy of cysteine 482. We conclude that the importance of cysteines in both agonist peptide and CaSR is due to a disulfide linkage between the two that is required for receptor activation by AMG 416.

Cysteine 482 has a non-essential role in normal CaSR function. Earlier studies using scanning mutagenesis of cysteines within the CaSR did not demonstrate activity dependent on cysteine 482 (Hu et al., 2001; Ray et al., 1999; Zhang et al., 2001). Native pCaSR is fully responsive to calcium and it is presumed that pigs are able to satisfy PTH control and other physiological demands with a CaSR that does not have cysteine at position 482.

Cysteine 482 is predicted to reside in a region of the CaSR that is believed to be intimately involved in receptor activation for Class C GPCRs. Most, but not all, of the known agonist interaction sites for the CaSR are mapped to the large ECD, and principally within the VFT domain (Khan and Conigrave, 2010; Zhang et al., 2014). Of exception is cinacalcet, a member of the phenylalkylamine class of calcimimetics, which is believed to bind within the heptahelical domain, and not within the ECD of the CaSR (Rodriguez et al., 2005). The VFT domain is characterized by two large lobes hinged together by three strands crossing between the lobes (**Figure 8**). X-ray crystallography of mGluR1 (Kunishima et al., 2000; Tsuchiya et al., 2002) and mGluR3 (Muto et al., 2007) and mutational analysis of TASR1 and TASR3 (Li, 2009; Zhang et al., 2010; Zhang et al., 2008) support a high affinity binding site for orthosteric ligands between the lobes and near the hinge of the VFT domain. Upon occupancy of Class C GPCR by orthosteric agonists, the hinge provides a flex point by which closure of the lobes is able to direct open and closed conformations in the protomeric receptor complex (Bessis et al., 2002; Kunishima et al., 2000; Tsuchiya et al., 2002). Closed conformations of the dimeric complex

MOL #98392

lead to receptor activation and initiation of signal transduction. Cysteine 482 is predicted to reside in the middle of the third hinge strand, in the interface between the two CaSR protomers. Whereas there is a cysteine in this location for the CaSR of most species (e.g., human, dog, mouse, rat, and rabbit) no other Class C GPCR have cysteines in this location. Due to the importance of cysteine 482 for AMG 416 activity, it is not expected that AMG 416 will have activity against other members of this GPCR family. In support of this, AMG 416 is inactive against the rat mGluR1 when overexpressed in HEK293T cells (Data on file, Amgen).

The observed in vivo pharmacology of AMG 416 supports rapid and readily reversible PDs, suggesting that the covalent disulfide bond between agonist peptide and the CaSR is labile and does not provide slow off rates. Following a 24-hour infusion of two different doses of AMG 416 in dogs, plasma PTH began to return to pre-infusion levels immediately upon cessation of infusion. The time to recovery of PTH levels toward baseline was inversely and principally correlated with AMG 416 plasma exposure levels and there were no unusual delays in PTH recovery. This is an expected behavior of a drug that is not tightly associated with the target, and would include one that exhibits a readily reversible covalent bond. Similar readily reversible PD behavior for AMG 416 has been shown in two other responsive species, human (Martin et al., 2014a; Martin et al., 2014b) and rat (Walter et al., 2014; Walter et al., 2013). The data support the concept of an environment at the parathyroid gland cell surface, which is balanced for reductive and oxidative modification of the cysteines in AMG 416 and position 482 of the CaSR.

In conclusion, the calcimimetic actions of AMG 416 are mediated through direct binding to the CaSR which leads to reductions in circulating levels of PTH as well as calcium. In responsive species, agonist peptide binding to the CaSR is mediated, in part, by a covalent disulfide bond between the D-cysteine in AMG 416 and cysteine 482 of the CaSR which appears to be labile in vivo as evidenced by readily reversible PDs. The AMG 416 binding site on the CaSR

MOL #98392

determined by cysteine 482 is separate from the binding sites for the orthosteric agonist calcium. Thus, binding of AMG 416 is topographically distinct from calcium, and AMG 416 is an allosteric activator of the CaSR.

MOL #98392

## **Acknowledgements**

The authors wish to thank Karen Pickthorn, Ph.D., Qun Yin, MS, Justin K. Murray, Ph.D., and Xiaochun Zhu, Ph.D. for their contributions to the research, and Holly Tomlin, MPH, and Margot Lisa Miglins, Ph.D. (employees and stockholders of Amgen Inc), for their medical writing assistance. All authors contributed to the drafting of the manuscript and approved the final version.

MOL #98392

### **Authorship Contributions**

Participated in research design: Alexander, Hunter, Walter, Baruch, Subramanian and Tomlinson

Conducted experiments: Alexander, Hunter, Dong, Subramanian, and Tomlinson

Contributed new reagents or analytic tools: Hunter and Tomlinson

Performed data analysis: Alexander, Hunter, Walter, Subramanian and Tomlinson

Wrote or contributed to the writing of the manuscript: Alexander, Hunter, Walter, Maclean, Baruch, Raju, and Tomlinson

MOL #98392

## References

- Bessis AS, Rondard P, Gaven F, Brabet I, Triballeau N, Prezeau L, Acher F and Pin JP (2002) Closure of the Venus flytrap module of mGlu8 receptor and the activation process: Insights from mutations converting antagonists into agonists. *Proc Natl Acad Sci U S A* **99**(17): 11097-11102.
- Block GA, Martin KJ, de Francisco AL, Turner SA, Avram MM, Suranyi MG, Hercz G, Cunningham J, Abu-Alfa AK and Messa P (2004a) Cinacalcet for secondary hyperparathyroidism in patients receiving hemodialysis. *N Engl J Med* **350**(15): 1516-1525.
- Block GA, Martin KJ, de Francisco AL, Turner SA, Avram MM, Suranyi MG, Hercz G, Cunningham J, Abu-Alfa AK, Messa P, Coyne DW, Locatelli F, Cohen RM, Evenepoel P, Moe SM, Fournier A, Braun J, McCary LC, Zani VJ, Olson KA, Drueke TB and Goodman WG (2004b) Cinacalcet for secondary hyperparathyroidism in patients receiving hemodialysis. *New England Journal of Medicine* **350**(15): 1516-1525.
- Breitwieser GE and Gama L (2001) Calcium-sensing receptor activation induces intracellular calcium oscillations. *Am J Physiol Cell Physiol* **280**(6): C1412-1421.
- Chen RA and Goodman WG (2004) Role of the calcium-sensing receptor in parathyroid gland physiology. *Am J Physiol Renal Physiol* **286**(6): F1005-1011.
- Conigrave AD and Hampson DR (2010) Broad-spectrum amino acid-sensing class C G-protein coupled receptors: molecular mechanisms, physiological significance and options for drug development. *Pharmacol Ther* **127**(3): 252-260.
- Conigrave AD, Mun HC, Delbridge L, Quinn SJ, Wilkinson M and Brown EM (2004) L-amino acids regulate parathyroid hormone secretion. *J Biol Chem* **279**(37): 38151-38159.

MOL #98392

Debe DA, Danzer JF, Goddard WA and Poleksic A (2006) STRUCTFAST: protein sequence remote homology detection and alignment using novel dynamic programming and profile-profile scoring. *Proteins* **64**(4): 960-967.

Felsenfeld AJ, Rodriguez M and Aguilera-Tejero E (2007) Dynamics of parathyroid hormone secretion in health and secondary hyperparathyroidism. *Clin J Am Soc Nephrol* **2**(6): 1283-1305.

Gincherman Y, Moloney K, McKee C and Coyne DW (2010) Assessment of adherence to cinacalcet by prescription refill rates in hemodialysis patients. *Hemodial Int* **14**(1): 68-72.

Goodman WG and Quarles LD (2008) Development and progression of secondary hyperparathyroidism in chronic kidney disease: lessons from molecular genetics. *Kidney Int* **74**(3): 276-288.

Hu J, Reyes-Cruz G, Goldsmith PK and Spiegel AM (2001) The Venus's-flytrap and cysteine-rich domains of the human Ca<sup>2+</sup> receptor are not linked by disulfide bonds. *J Biol Chem* **276**(10): 6901-6904.

Hu J and Spiegel AM (2007) Structure and function of the human calcium-sensing receptor: insights from natural and engineered mutations and allosteric modulators. *J Cell Mol Med* **11**(5): 908-922.

Huang Y, Zhou Y, Castiblanco A, Yang W, Brown EM and Yang JJ (2009) Multiple Ca(2+)-binding sites in the extracellular domain of the Ca(2+)-sensing receptor corresponding to cooperative Ca(2+) response. *Biochemistry* **48**(2): 388-398.

Huang Y, Zhou Y, Yang W, Butters R, Lee HW, Li S, Castiblanco A, Brown EM and Yang JJ (2007) Identification and dissection of Ca(2+)-binding sites in the extracellular domain of Ca(2+)-sensing receptor. *J Biol Chem* **282**(26): 19000-19010.

IUPHAR/BPS Guide to Pharmacology: G Protein-Coupled Receptors (2014) G Protein-Coupled Receptor List. <http://www.guidetopharmacology.org/GRAC/GPCRListForward?class=C>.

MOL #98392

Khan MA and Conigrave AD (2010) Mechanisms of multimodal sensing by extracellular Ca(2+)-sensing receptors: a domain-based survey of requirements for binding and signalling. *Br J Pharmacol* **159**(5): 1039-1050.

Kidney Disease: Improving Global Outcomes (KDIGO) CKD-MBD Work Group (2009) KDIGO clinical practice guideline for the diagnosis, evaluation, prevention, and treatment of Chronic Kidney Disease-Mineral and Bone Disorder (CKD-MBD). *Kidney Int Suppl*(113): S1-130.

Komaba H, Goto S, Fujii H, Hamada Y, Kobayashi A, Shibuya K, Tominaga Y, Otsuki N, Nibu K, Nakagawa K, Tsugawa N, Okano T, Kitazawa R, Fukagawa M and Kita T (2010) Depressed expression of Klotho and FGF receptor 1 in hyperplastic parathyroid glands from uremic patients. *Kidney Int* **77**(3): 232-238.

Kunishima N, Shimada Y, Tsuji Y, Sato T, Yamamoto M, Kumasaka T, Nakanishi S, Jingami H and Morikawa K (2000) Structural basis of glutamate recognition by a dimeric metabotropic glutamate receptor. *Nature* **407**(6807): 971-977.

Li X (2009) T1R receptors mediate mammalian sweet and umami taste. *Am J Clin Nutr* **90**(3): 733S-737S.

Lindberg JS, Culleton B, Wong G, Borah MF, Clark RV, Shapiro WB, Roger SD, Husserl FE, Klassen PS, Guo MD, Albizem MB and Coburn JW (2005) Cinacalcet HCl, an oral calcimimetic agent for the treatment of secondary hyperparathyroidism in hemodialysis and peritoneal dialysis: a randomized, double-blind, multicenter study. *J Am Soc Nephrol* **16**(3): 800-807.

Martin KJ, Bell G, Pickthorn K, Huang S, Vick A, Hodsman P and Peacock M (2014a) Velcalcetide (AMG 416), a novel peptide agonist of the calcium-sensing receptor, reduces serum parathyroid hormone and FGF23 levels in healthy male subjects. *Nephrol Dial Transplant* **29**(2): 385-392.



MOL #98392

Martin KJ, Pickthorn K, Huang S, Block GA, Vick A, Mount PF, Power DA and Bell G (2014b)

AMG 416 (velcalcetide) is a novel peptide for the treatment of secondary hyperparathyroidism in a single-dose study in hemodialysis patients. *Kidney Int* **85**(1): 191-197.

Moe SM, Chertow GM, Coburn JW, Quarles LD, Goodman WG, Block GA, Drueke TB,

Cunningham J, Sherrard DJ, McCary LC, Olson KA, Turner SA and Martin KJ (2005) Achieving NKF-K/DOQI bone metabolism and disease treatment goals with cinacalcet HCl. *Kidney International* **67**(2): 760-771.

Mundy GR and Guise TA (1999) Hormonal control of calcium homeostasis. *Clin Chem* **45**(8 Pt 2): 1347-1352.

Muto T, Tsuchiya D, Morikawa K and Jingami H (2007) Structures of the extracellular regions of the group II/III metabotropic glutamate receptors. *Proc Natl Acad Sci U S A* **104**(10): 3759-3764.

National Kidney Foundation (2003) National Kidney Foundation (2003) K/DOQI clinical practice guidelines for bone metabolism and disease in chronic kidney disease. *Am J Kidney Dis* **42**(4 Suppl 3): S1-201.

Nemeth EF, Steffey ME, Hammerland LG, Hung BC, Van Wagenen BC, DelMar EG and

Balandrin MF (1998) Calcimimetics with potent and selective activity on the parathyroid calcium receptor. *Proc Natl Acad Sci U S A* **95**(7): 4040-4045.

Padhi D and Harris R (2009) Clinical pharmacokinetic and pharmacodynamic profile of cinacalcet hydrochloride. *Clin Pharmacokinet* **48**(5): 303-311.

Pawson AJ, Sharman JL, Benson HE, Faccenda E, Alexander SP, Buneman OP, Davenport

AP, McGrath JC, Peters JA, Southan C, Spedding M, Yu W, Harmar AJ and Nc I (2014) The IUPHAR/BPS Guide to PHARMACOLOGY: an expert-driven knowledgebase of drug targets and their ligands. *Nucleic Acids Res* **42**(Database issue): D1098-1106.

MOL #98392

Ray K, Hauschild BC, Steinbach PJ, Goldsmith PK, Hauache O and Spiegel AM (1999)

Identification of the cysteine residues in the amino-terminal extracellular domain of the human Ca(2+) receptor critical for dimerization. Implications for function of monomeric Ca(2+) receptor. *J Biol Chem* **274**(39): 27642-27650.

Rodriguez M, Nemeth E and Martin D (2005) The calcium-sensing receptor: a key factor in the pathogenesis of secondary hyperparathyroidism. *Am J Physiol Renal Physiol* **288**(2): F253-264.

Sensipar Prescribing Information [Amgen Inc.].

Tfelt-Hansen J and Brown EM (2005) The calcium-sensing receptor in normal physiology and pathophysiology: a review. *Critical Reviews in Clinical Laboratory Sciences* **42**(1): 35-70.

Tsuchiya D, Kunishima N, Kamiya N, Jingami H and Morikawa K (2002) Structural views of the ligand-binding cores of a metabotropic glutamate receptor complexed with an antagonist and both glutamate and Gd3+. *Proc Natl Acad Sci U S A* **99**(5): 2660-2665.

Walter S, Baruch A, Alexander ST, Janes J, Sho E, Dong J, Yin Q, Maclean D, Mendel DB, Karim F and Johnson RM (2014) Comparison of AMG 416 and cinacalcet in rodent models of uremia. *BMC Nephrol* **15**: 81.

Walter S, Baruch A, Dong J, Tomlinson JE, Alexander ST, Janes J, Hunter T, Yin Q, Maclean D, Bell G, Mendel DB, Johnson RM and Karim F (2013) Pharmacology of AMG 416 (Velcalcetide), a novel peptide agonist of the calcium-sensing receptor, for the treatment of secondary hyperparathyroidism in hemodialysis patients. *J Pharmacol Exp Ther* **346**(2): 229-240.

Wei Y, Li L, Wang D, Zhang CY and Zen K (2014) Importin 8 regulates the transport of mature microRNAs into the cell nucleus. *J Biol Chem* **289**(15): 10270-10275.

Zhang C, Huang Y, Jiang Y, Mulpuri N, Wei L, Hamelberg D, Brown EM and Yang JJ (2014) Identification of an L-phenylalanine binding site enhancing the cooperative responses of the calcium-sensing receptor to calcium. *J Biol Chem* **289**(8): 5296-5309.

MOL #98392

Zhang F, Klebansky B, Fine RM, Liu H, Xu H, Servant G, Zoller M, Tachdjian C and Li X (2010)

Molecular mechanism of the sweet taste enhancers. *Proc Natl Acad Sci U S A* **107**(10): 4752-4757.

Zhang F, Klebansky B, Fine RM, Xu H, Pronin A, Liu H, Tachdjian C and Li X (2008) Molecular

mechanism for the umami taste synergism. *Proc Natl Acad Sci U S A* **105**(52): 20930-20934.

Zhang Z, Qiu W, Quinn SJ, Conigrave AD, Brown EM and Bai M (2002) Three adjacent serines

in the extracellular domains of the CaR are required for L-amino acid-mediated potentiation of receptor function. *J Biol Chem* **277**(37): 33727-33735.

Zhang Z, Sun S, Quinn SJ, Brown EM and Bai M (2001) The extracellular calcium-sensing

receptor dimerizes through multiple types of intermolecular interactions. *J Biol Chem* **276**(7): 5316-5322.

MOL #98392

## Footnotes

This work was supported by KAI Pharmaceuticals, a wholly owned subsidiary of Amgen, Thousand Oaks, California.

Part of this work was presented at The 2nd International Symposium on the Calcium-sensing Receptor", San Diego, CA, March 3-4, 2015

Shawn T. Alexander, Amgen Inc, 1120 Veterans Boulevard, South San Francisco, CA 94080

Email: shawna@amgen.com.

MOL #98392

## Legends for Figures

**Figure 1.** Stimulation of hCaSR requires a cysteine in the agonist peptide. (A) Molecular structures with atomic details of the side chain of d-cysteine for three synthetic peptides selected to help elucidate the critical components required for hCaSR activation. (B) CaSR activation in a heterologous expression system. Stable HEK293T cell line expressing hCaSR was incubated with the orthosteric CaSR agonist, calcium alone [●]; or with increasing concentrations of a cysteine-containing peptide (KP-2067 [■]; n = 4), or a homologue lacking cysteine (KP-2140 [◇]; n = 4), both in the presence of 1.2 mM calcium. CaSR activity was determined by quantifying IP-1, a measure of Gq activation. (C) Suppression of PTH secretion, a primary pharmacodynamic measure of in vivo CaSR stimulation. Normal Sprague Dawley rats were administered IV bolus injections of [■] saline (n = 22); [●] 0.5 mg/kg KP-2067 (n = 5); [○] 3 mg/kg KP-2067 (n = 5); or [▼] 3 mg/kg KP-2140 (n = 5). Plasma PTH levels were measured over 4 hours and normalized to pre-dose values for each animal. Mean ± S.E.M..

**Figure 2.** IV Bolus administration of AMG 416 in the dog and the pig. (A, B) Dogs were administered a single IV bolus AMG 416: [●] 1.5 mg/kg AMG 416 (n = 4). (A) Log plasma concentration of AMG 416 (ng/mL) and (B) total calcium (mg/dL) were measured over 48 hours. Mean ± S.E.M.. (C, D) Pigs were administered a single IV bolus of AMG 416: [□] 0.3 mg/kg (n = 3); [▲] 1.0 mg/kg (n = 3); or [■] 5.0 mg/kg (n = 5). (C) Log plasma concentration of AMG 416 (ng/mL) and (D) total calcium (mg/dL) were measured over 48 hours. Mean ± S.E.M. for 0.3 mg/kg and 1.0 mg/kg.

**Figure 3.** Response to activation of native and point mutant hCaSR by the orthosteric agonist calcium and agonist peptides. IP-1, a measure of Gq activation, was quantified. Transiently transfected HEK293T cells: [■, □], native human (Cys482) CaSR cells (n = 4); [●, ○], mutant

MOL #98392

human Ser482 CaSR cells (n = 4); and [▲, Δ], mutant human Tyr482 CaSR cells (n = 4) were stimulated: (A) with 1.2 mM calcium (closed symbols) or no calcium added (open symbols). Mean ± S.E.M. shown; (B) in the presence of 1.2 mM calcium either with (closed symbols) or without (open symbols) agonist peptide KP-2067 (n = 4; mean ± S.E.M.); (C) in the presence of 1.2 mM calcium either with (closed symbols) or without (open symbols) agonist peptide AMG 416 (n=2; mean ± S.E.M.).

**Figure 4.** Response to activation of native and point mutant pCaSR by the orthosteric agonist calcium and agonist peptides. IP-1, a measure of Gq activation, was quantified. Transiently transfected HEK293T cells: [■, □], native human (Cys482) CaSR cells (n = 4); [●, ○], native pig (Y482) CaSR cells (n = 4); and mutant human Ser482 CaSR cells (n = 4); and [▲, Δ], mutant pig Cys482 CaSR cells (n = 4) were stimulated: (A) with 1.2 mM calcium (closed symbols) or no calcium added (open symbols); (B) in the presence of 1.2 mM calcium either with (closed symbols) or without (open symbols) agonist peptide KP-2067 (n = 4); (C) in the presence of 1.2 mM calcium either with (closed symbols) or without (open symbols) agonist peptide AMG 416 (n=2). Mean ± S.E.M. shown.

**Figure 5.** Collision induced dissociation MS/MS spectra of acrylamide- and KP-2067-modified CaSR peptide (<sup>480</sup>DECGD<sup>485</sup>L) conjugates. (A) Secondary MS spectrum of *m/z* 722.3 (+1 charge) precursor ion from acrylamide-modified DECGDL; (B) Secondary MS spectrum of *m/z* 789.9 (+2 charge) precursor ion from KP-2067/ DECGDL conjugate. Proposed fragment assignments are shown in insets in each panel. The charge state of each fragment ion is shown in parentheses. Amino acids labels are shown in bold; lower and upper case letters represent D- and L-amino acids, respectively.

MOL #98392

**Figure 6.** Twenty-four hour IV infusion of AMG 416 in the dog. Dogs were infused with AMG 416 at [□], 0.192 mg/kg (n = 4) or [■], 0.480 mg/kg (n = 4), or with [▲], vehicle. (A) Log plasma concentration of AMG 416 (ng/mL), (B) plasma PTH (pg/mL), and (C) total calcium (mg/dL) were measured over 48 hours. Mean ± S.E.M. shown.

**Figure 7.** Alignment of the Cysteine 482 region in CaSR with all human GPCR having VFT. Alignment was initially generated using full length primary amino acid sequences from each human GPCR with a known VFT, and refined based on X-ray crystallography structures from 4 class C members (RCSB Protein Data Bank: mGluR1, PDB ID: 1EWT, 1EWK; mGluR3, PDB ID: 2E4U, 3SM9; mGluR5, PDB ID: 3LMK; mGluR7, PDB ID: 3MQ4). Refer to numbers at the top of alignment for what follows. Columns 1, 3, 5, and 7 highlight (boxes) landmarks from known X-ray structures. Open boxes within column 1 mark the start, and within column 7 mark the end of the hinge 3 strand within each structure. Gray broken boxes (3, 5) represent amino acids in the only two turns in each hinge 3 strand. Columns 2, 4 and 6 highlight highly conserved residues within each hinge strand and with similar distances to x-ray determined landmarks at 1, 3, 5 and 7. Highly conserved phenylalanines (columns 2, 4) as well as a largely conserved Glycine-anionic dipeptide patch (column 6) are also highlighted.

**Figure 8.** Snapshots of key elements in a structural model for hCaSR: subdomain structure of the ECD, hinge region in the VFT and position of Cysteine 482. Model was developed using the StructFast™ algorithm (Eidogen-Sertanty, Inc, Oceanside, CA) (Debe et al., 2006) based on the structure of mGluR3 (Muto et al., 2007; PDB ID: 2E4U), and displayed with PyMOL (Molecular Graphics System, Version 1.3, Schrödinger, LLC). (A) High level perspective of entire ECD of the hCaSR viewed along the cell surface. Black residues, Lobe 1 of VFT; light blue residues, Lobe 2 of VFT; brown residues, cysteine rich subdomain; yellow residues, hinge strand 1 in VFT (amino acid 167-189); magenta residues, hinge strand 2 in VFT (amino acid 323-327); orange-

MOL #98392

brown residues, hinge strand 3 in VFT (amino acid 466-489); Green residue is cysteine 482.

(B) Zoom view with same perspective as in (A).



MOL #98392

**Table 1. Unique Pig Residues within the VFT Subdomain of the pCaSR ECD**

Position	Amino Acid Residues			
	Human	Dog	Rat	Pig
50	Aspartate	Aspartate	Aspartate	Glutamate
52	Lysine	Lysine	Lysine	Glutamate
340	Arginine	Arginine	Arginine	Serine
369	Proline	Serine	Proline	Threonine
370	Valine	Methionine	Valine	Threonine
438	Leucine	Leucine	Leucine	Isoleucine
471	Asparagine	Asparagine	Asparagine	Serine
482	Cysteine	Cysteine	Cysteine	Tyrosine
486	Valine	Methionine	Valine	Alanine

Human, dog and rat CaSR sequences were obtained from the public database (NCBI:

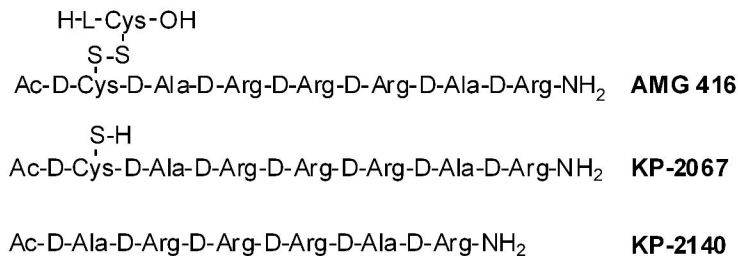
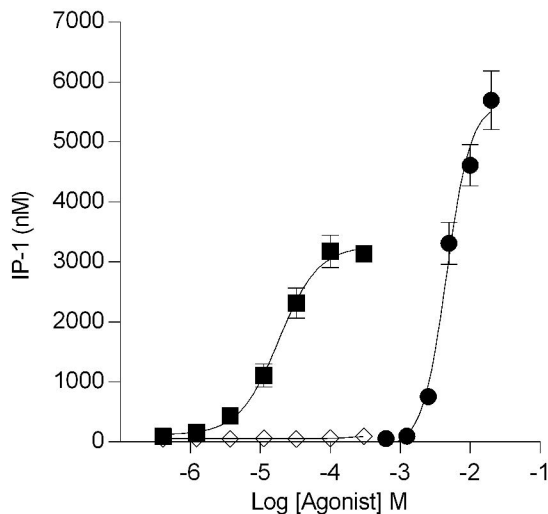
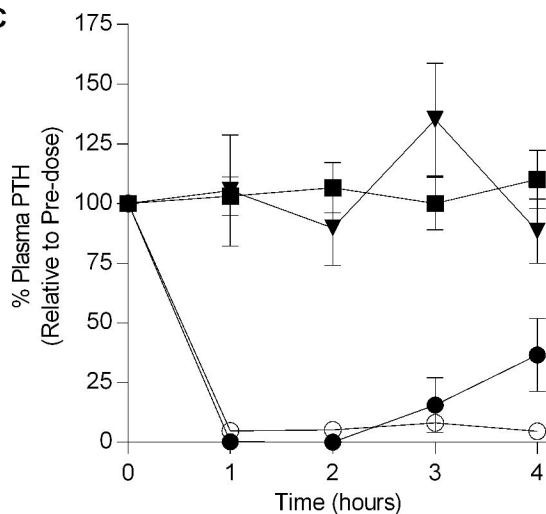
<http://www.ncbi.nlm.nih.gov/homologene/332>

MOL #98392

**Table 2. Fractional binding of KP-2067 to CaSR Cysteine 482 in HEK293 cells expressing human calcium-sensing receptor (n=4)**

KP-2067 μM	Mean Percent Bound
0	ND
8	ND
25	5.3 ± 3.2 <sup>a</sup>
80	12.1 ± 4.4 <sup>a</sup>

ND = Not detected; <sup>a</sup> S.E.M.

**A****B****C****Figure 1**

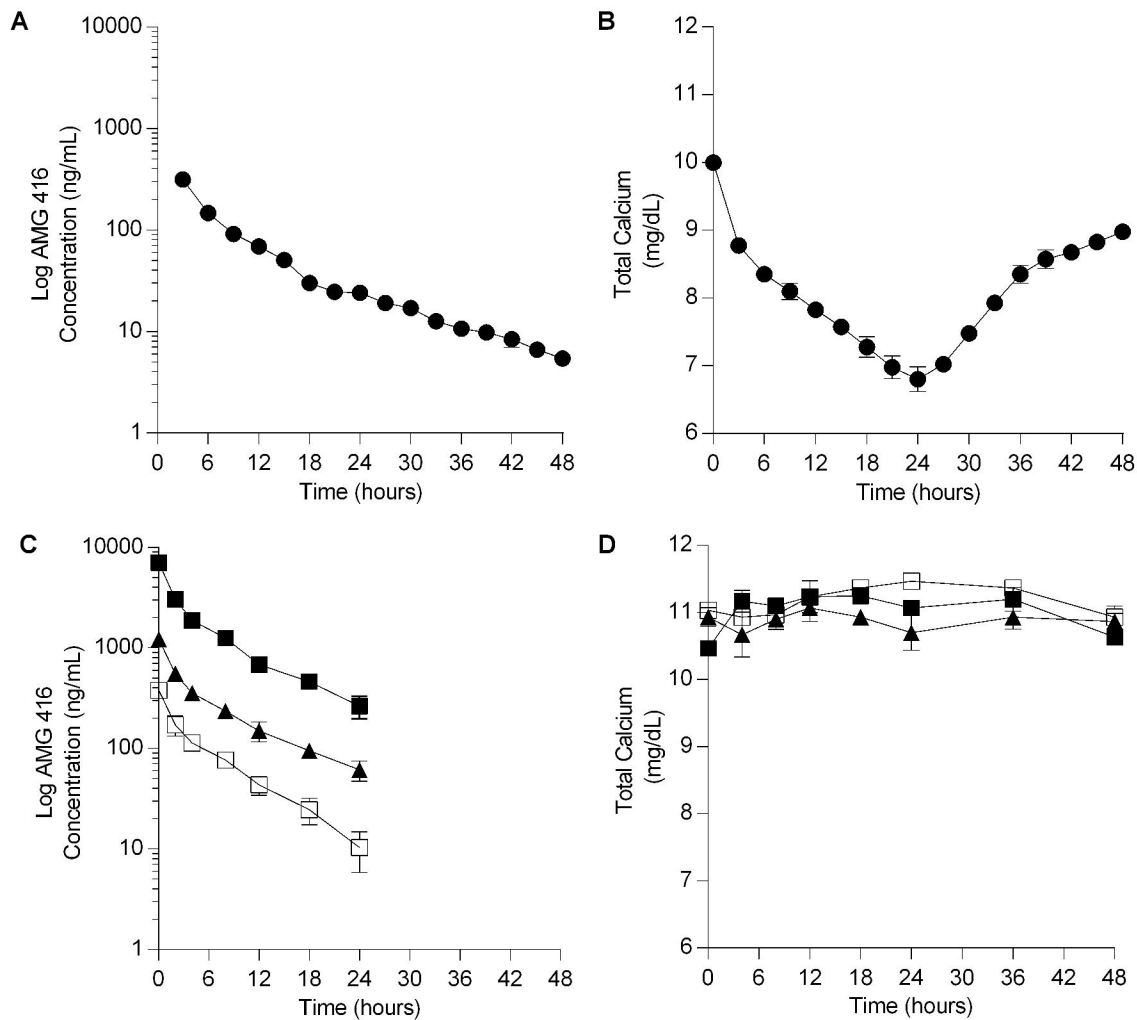


**Figure 2**

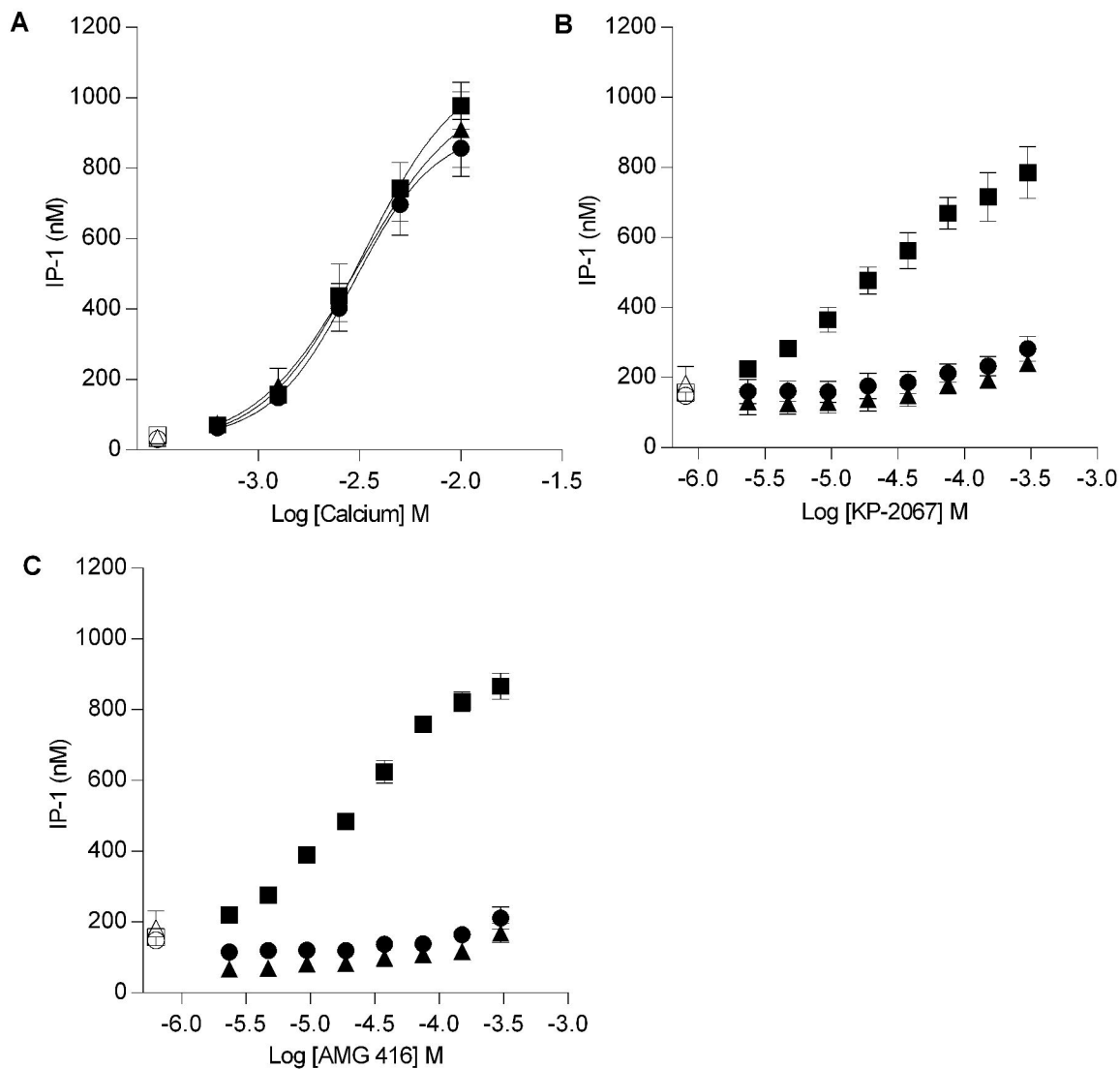


**Figure 3**

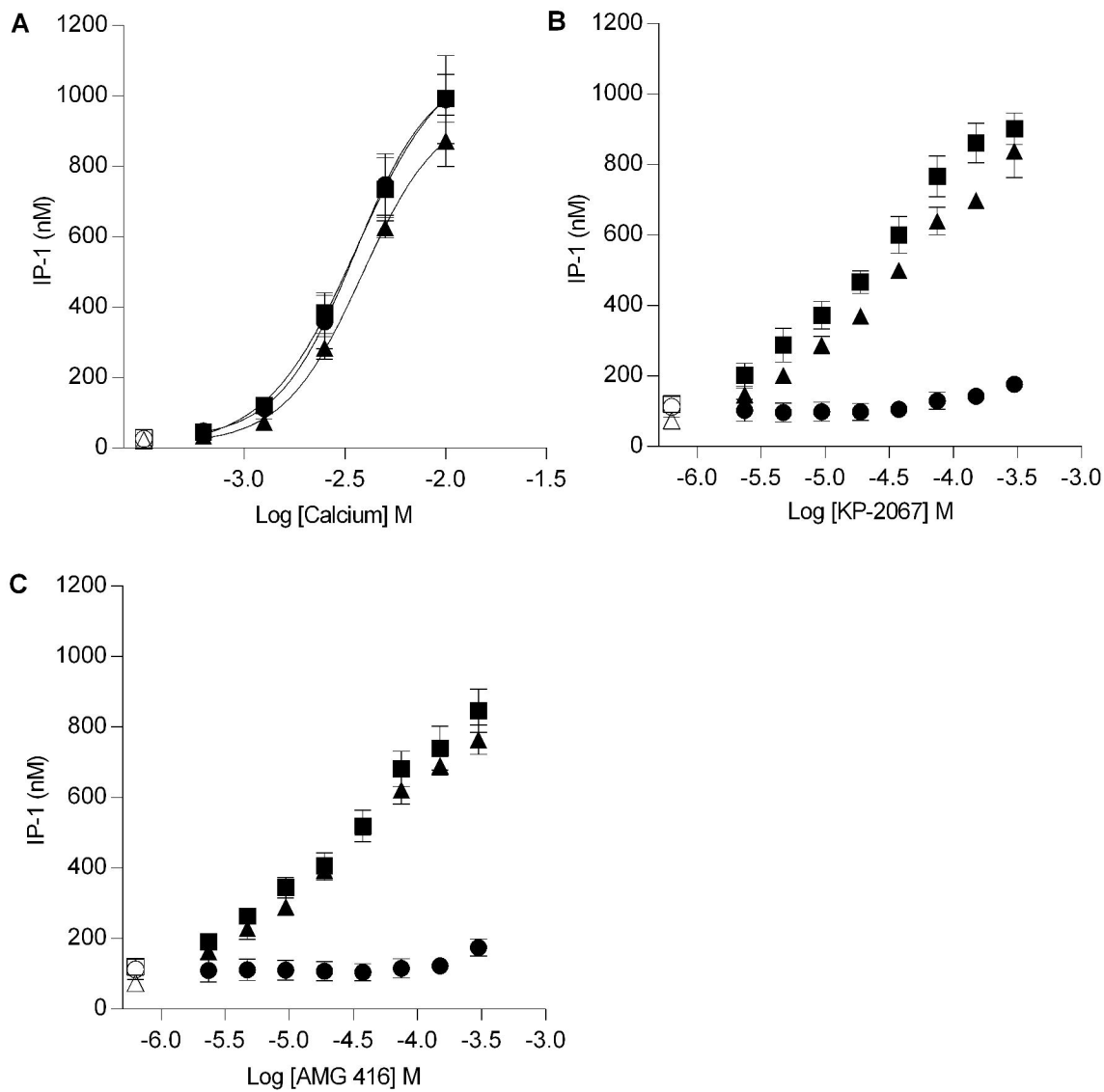


**Figure 4**

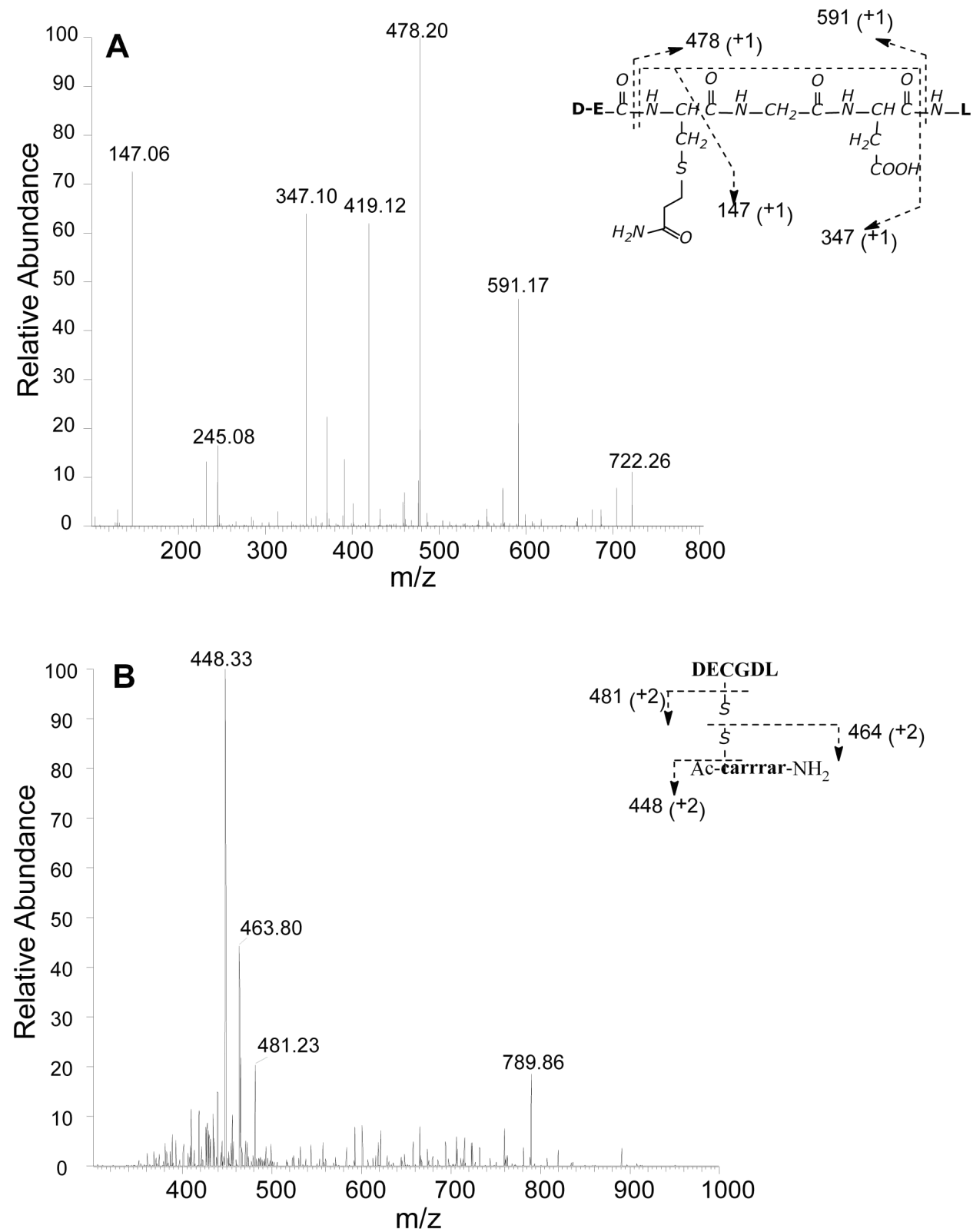
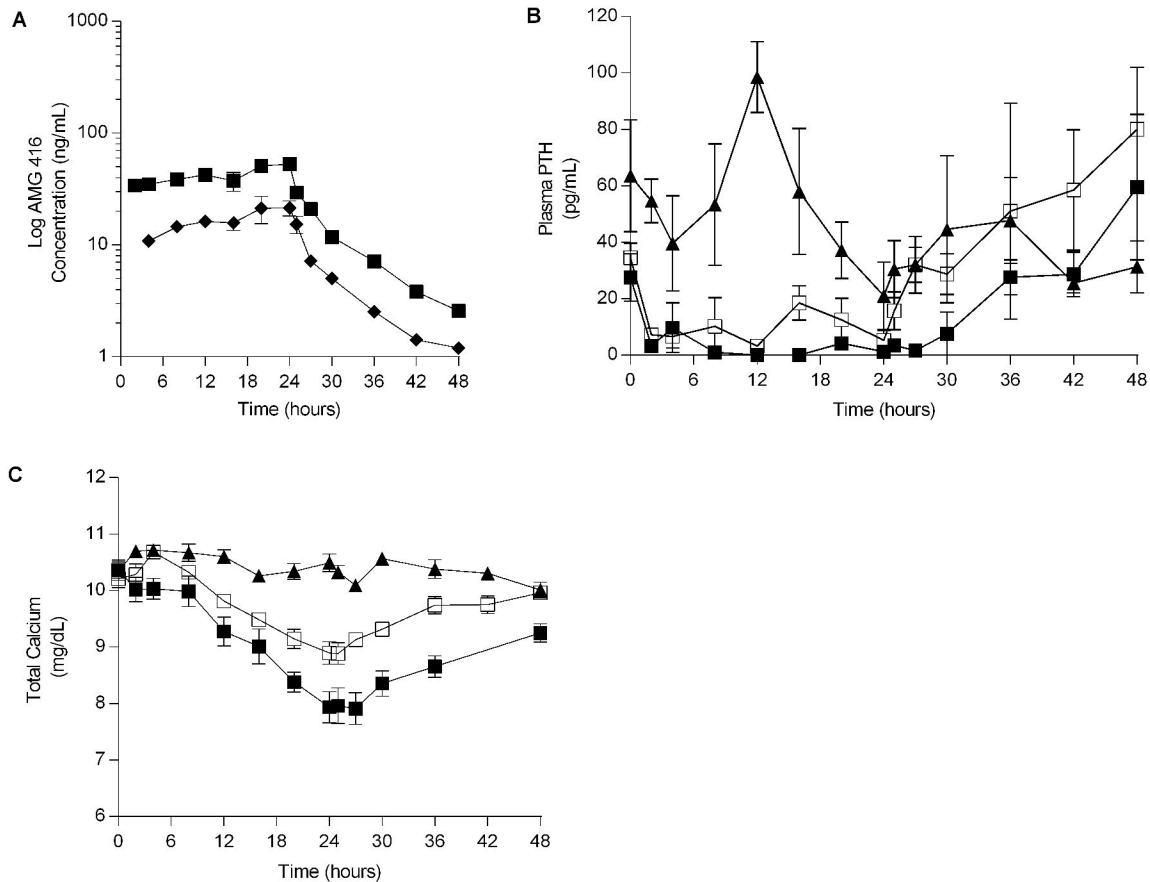


Figure 5



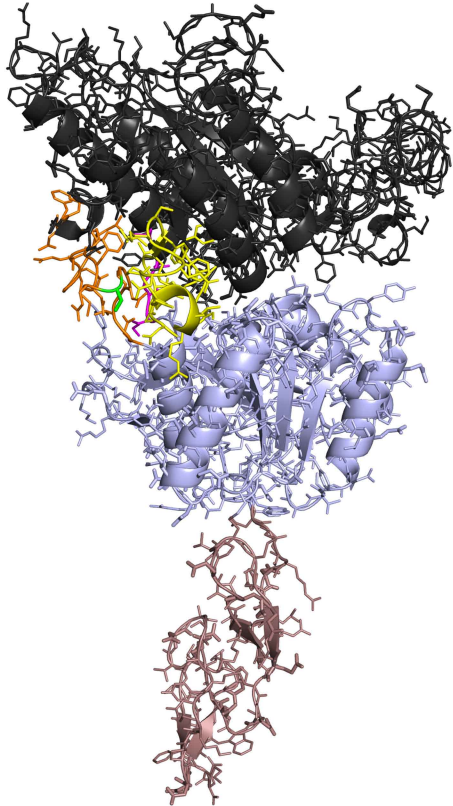
**Figure 6**



		1	2		3		4	5	6		7	
CaSR	462	K - HLRHLNFT	N - - - - - NMG	EQVTFDEC	GD	LVGNYS	I I NW	494				
GPRC6A	448	G - VLKNVTFT	D - - - - - GWN	S - FHFDAH	GD	LNTGYDV	V LW	479				
mGluR1	452	- DFL I <b>KSS</b> FI	G - - - - - <b>VSG</b>	EEVWFDE <b>EKG</b>	GD	APGR <b>RY</b> D	I MNL	484				
mGluR2	420	KDFVLNVKFD	APFRP - ADTH	NEVRFD	DRFGD	G I GRYN	I FTY	458				
mGluR3	432	KDYLL <b>KI</b> NFT	APFNPNK <b>DAD</b>	S I VKFD	<b>DTF</b> GD	GMGR <b>RY</b> N	V FNF	471				
mGluR4	448	K - Y I RNVNFS	G - - - - - I AG	NPVTFN	ENG	GD	APGRYD	I YQY	480			
mGluR5	439	- ESLM <b>KT</b> NFT	G - - - - - <b>VSG</b>	DT I L F D	<b>EN</b> GD	SPGR <b>RY</b> E	I MNF	471				
mGluR6	443	Q - Y I RAVRFN	G - - - - - SAG	TPVMFN	ENG	GD	APGRYD	I FQY	475			
mGluR7	450	K - Y I R <b>NV</b> NFN	G - - - - - <b>SAG</b>	TPVMFN	<b>KN</b> GD	APGR <b>RY</b> D	I FQY	482				
mGluR8	444	G - Y I RAVNFN	G - - - - - SAG	TPVTFN	ENG	GD	APGRYD	I FQY	476			
TAS1R1	423	EQ - I HKVHFL	- - - - - - LHK	DTVAFND	NRD	PLSSYN	I I AW	454				
TAS1R2	422	EE - IWKVNFT	- - - - - - LLD	HQ I F F D	PQGD	VALHLE	I VQW	453				
TAS1R3	428	EN - MYNLT FH	- - - - - - VGG	LPLRFD	SSGN	VDMEYD	L KLW	459				
GABA B1	510	YRAMNSSSFE	G - - - - - - VS	GHVVFD	ASGS	RMAWT	L I EQL	542				
GABA B2	400	LNAMNETNFF	G - - - - - - VT	GQVVF	- RGE	RMGT I	K FTQF	431				

Figure 7

A



B

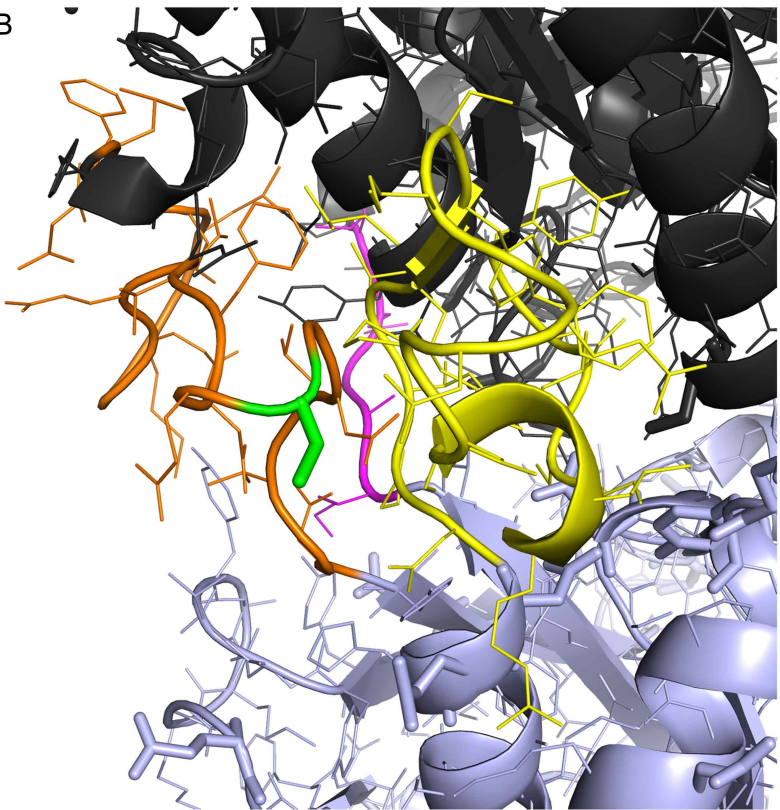


Figure 8